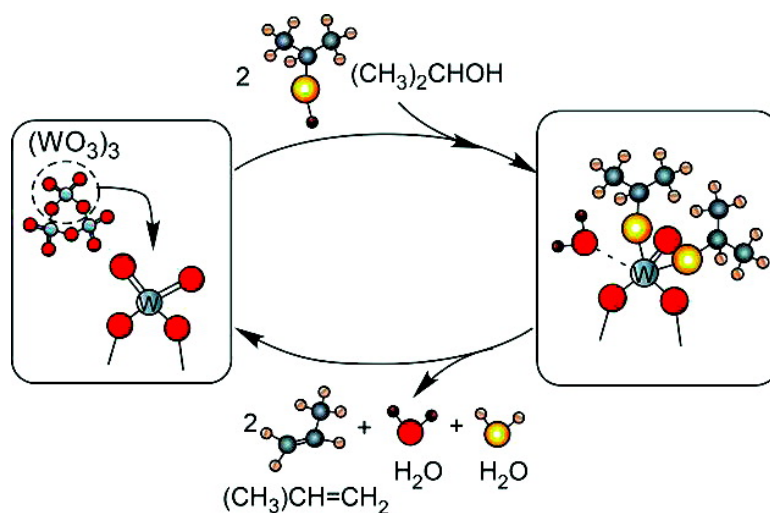


## Catalytic Dehydration of 2-Propanol on (WO) Clusters on TiO(110)

Yu Kwon Kim, Roger Rousseau, Bruce D. Kay, J. M. White, and Zdenek Dohnálek

*J. Am. Chem. Soc.*, **2008**, 130 (15), 5059-5061 • DOI: 10.1021/ja800730g • Publication Date (Web): 25 March 2008

Downloaded from <http://pubs.acs.org> on February 8, 2009



### More About This Article

Additional resources and features associated with this article are available within the HTML version:

- Supporting Information
- Links to the 1 articles that cite this article, as of the time of this article download
- Access to high resolution figures
- Links to articles and content related to this article
- Copyright permission to reproduce figures and/or text from this article

[View the Full Text HTML](#)

## Catalytic Dehydration of 2-Propanol on $(\text{WO}_3)_3$ Clusters on $\text{TiO}_2(110)$

Yu Kwon Kim,<sup>†</sup> Roger Rousseau,<sup>\*,‡</sup> Bruce D. Kay,<sup>\*,‡</sup> J. M. White,<sup>†,‡,#</sup> and Zdenek Dohnálek<sup>\*,‡</sup>

Department of Chemistry and Biochemistry, Center for Materials Chemistry, University of Texas at Austin, Texas 78712, and Pacific Northwest National Laboratory, Fundamental Sciences Directorate and Institute for Interfacial Catalysis, Richland, Washington 99352

Received January 29, 2008; E-mail: zdenek.dohnalek@pnl.gov

Monodispersed clusters with well-defined structure are an excellent platform for model catalytic studies. Ultimately, they can provide a detailed understanding of site-specific reactivity and yield structure–reactivity relationships that cannot be obtained otherwise. Our work in this area focuses on early transition-metal oxide catalysts which are of particular technological importance and have broad applications in partial oxidation of alcohols, oxidative dehydrogenation of hydrocarbons, and selective reduction of nitric oxide.<sup>1–4</sup> Recently, we reported on the preparation of monodispersed tungsten trioxide trimers,  $(\text{WO}_3)_3$ , via direct evaporation of  $\text{WO}_3$  solid onto rutile  $\text{TiO}_2(110)$ .<sup>5,6</sup> Studies of gas-phase tungsten oxide clusters indicate that the  $(\text{WO}_3)_3$  trimer has a cyclic ring structure as schematically shown in Figure 1.<sup>7–9</sup>

In this study we use temperature programmed desorption (TPD) and density functional theory (DFT) calculations to investigate the catalytic properties of monodispersed  $(\text{WO}_3)_3$  clusters. Our results show that the clusters provide an extremely efficient dehydration reaction channel for alcohols, which utilizes both strong Lewis acid  $\text{W(VI)}$  sites and doubly bonded oxygen tungstyl ( $\text{W}=\text{O}$ ) groups. For this specific reaction, the activation energy for the dehydration is practically unaffected by the cluster proximity and/or binding to  $\text{TiO}_2(110)$ . Our results are particularly interesting in that the dominant Lewis acid–based activity of the  $(\text{WO}_3)_3$  cluster with no support effect contrasts strikingly with the Bronsted acid–based activity of most high surface area  $\text{WO}_x$ -based supported catalysts, which are believed to be strongly affected by the support oxide.<sup>1,2</sup>

The experiments were carried out in an ultrahigh vacuum (UHV) molecular beam scattering chamber ( $7 \times 10^{-11}$  Torr) described previously.<sup>12</sup> A rutile  $\text{TiO}_2(110)$  crystal ( $10 \times 10 \times 1$  mm<sup>3</sup>, Princeton Scientific) was cleaned by repeated cycles of  $\text{Ne}^+$  sputtering and annealing to 850–900 K.<sup>10,11</sup> A high temperature effusion cell (CreaTec) was used to evaporate  $\text{WO}_3$  (99.95% Aldrich) and generate  $(\text{WO}_3)_3$  gas phase clusters.<sup>7,8</sup> The  $(\text{WO}_3)_3$  flux was monitored using a quartz crystal microbalance (Inficon). Deposited  $(\text{WO}_3)_3$  was removed from  $\text{TiO}_2(110)$  by  $\text{Ne}^+$  sputtering at 500 K and annealing at 850–900 K. 2-Propanol was purified with repeated freeze–pump–thaw cycles and dosed using an effusive molecular beam. TPD measurements (ramp rate of 1.8 K/sec) were performed using a quadrupole mass spectrometer (UTI). Mass fragments for 2-propanol, water, hydrogen, propene, acetone, and isopropyl ether were followed to identify all plausible reaction products.<sup>10,11</sup>

All calculations were carried out employing DFT with a gradient-corrected functional for exchange and correlation<sup>13</sup> as implemented in the CP2K package.<sup>14,15</sup> Core–electrons are modeled as norm-

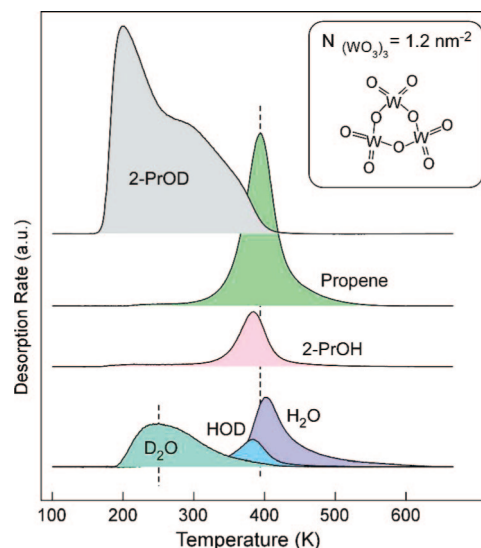


**Figure 1.** TPD spectra of 2-propanol ( $(\text{CH}_3)_2\text{CHOD}$  tracked at 46 amu and  $(\text{CH}_3)_2\text{CHOH}$  at 45 amu), propene (41 amu), and water (18, 19, and 20 amu) after  $5.2 \text{ nm}^{-2}$   $(\text{CH}_3)_2\text{CHOD}$  exposure<sup>10,11</sup> dosed on  $1.2 \text{ nm}^{-2}$   $(\text{WO}_3)_3$  clusters deposited on  $\text{TiO}_2(110)$  at 100 K. The contributions of 2-propanol in 18, 19, 20, and 41 amu were subtracted using a fragmentation pattern determined from 2-propanol multilayer desorption.<sup>10,11</sup> The integrated area of  $\text{D}_2\text{O}$  and  $\text{H}_2\text{O}$  are found to be the same within 10% and are proportional to the  $(\text{WO}_3)_3$  coverage.

conserving pseudopotentials and the wave functions expanded in a double- $\zeta$  Gaussian basis set with a planewave auxiliary basis of 300 Ry energy cutoff, and the  $\Gamma$ -point for Brillouin zone integration. Calculation of all reaction coordinates were performed with the nudged-elastic-band method (NEB)<sup>16</sup> employing 8–20 beads depending on the complexity of the rearrangement. The reaction coordinate for each reaction in our mechanism, as obtained from NEB, were verified by normal-mode analysis of the transition state to determine that it represented a saddle point on the potential energy surface. All surface reactions are modeled on a  $(4 \times 2)$  rutile- $\text{TiO}_2(110)$  surface slab of 4  $\text{TiO}_2$  units depth.

Figure 1 shows the TPD spectra of propene and water formed during the reaction of monodeuterated 2-propanol- $d_1$ ,  $(\text{CH}_3)_2\text{CHOD}$ , with  $(\text{WO}_3)_3$  clusters deposited on  $\text{TiO}_2(110)$  at 100 K. The unreacted  $(\text{CH}_3)_2\text{CHOD}$ , as well as  $(\text{CH}_3)_2\text{CHOH}$  formed during the reaction via H/D exchange are also shown. The unreacted  $(\text{CH}_3)_2\text{CHOD}$  desorbs between 170 and 400 K. The desorption of the first reaction product,  $\text{D}_2\text{O}$ , extends from 200 to 350 K with maximum rate at 250 K. This indicates that the O–D bond in  $(\text{CH}_3)_2\text{CHO–D}$  has been cleaved yielding  $\text{D}_2\text{O}(\text{g})$  via recombinative ( $\text{OD} + \text{D}$ ) desorption. The absence of  $\text{H}_2\text{O}$  and HDO in this range shows that no C–H bonds have been cleaved below  $\sim 350$  K. The oxygen atom in  $\text{D}_2\text{O}(\text{g})$  is likely from the

<sup>†</sup> University of Texas at Austin.

<sup>‡</sup> Fundamental Sciences Directorate and Institute for Interfacial Catalysis.

<sup>#</sup> Deceased August 31, 2007.

(WO<sub>3</sub>)<sub>3</sub> cluster since the oxygen from the alcohol is not available until further decomposition of the alkoxy group. While we do not have direct evidence for oxygen scrambling between alcohol and the cluster, we have observed <sup>16</sup>O/<sup>18</sup>O exchange after the adsorption and dissociation of isotopically labeled H<sub>2</sub><sup>18</sup>O on (W<sup>16</sup>O<sub>3</sub>)<sub>3</sub> clusters (not shown).

The primary product of interest, propene, CH<sub>3</sub>CH=CH<sub>2</sub>, desorbs via first order kinetics with a peak desorption at 400 K. Since physisorbed CH<sub>3</sub>CH=CH<sub>2</sub> desorbs below 100 K (data not shown) the desorption has to be limited by C–O and/or C–H bond cleavage. Preliminary data for the dehydration of ethanol, 2-propanol, *t*-butyl alcohol, show a clear linear relationship between the dehydration temperature and the inductive effect of alkyl substituents as previously observed for the dehydration of alcohols on clean TiO<sub>2</sub>(110).<sup>11,17</sup> This correlation strongly indicates that C–O bond cleavage is the rate limiting step. The H<sub>2</sub>O desorption closely follows the propene desorption indicating that the C–H bond cleavage participates in the same transition state. Further evidence is provided by kinetic H/D isotope effect observed in the experiments with (CD<sub>3</sub>)<sub>2</sub>CDOD, where CD<sub>3</sub>CD=CD<sub>2</sub> desorbs at a temperature ~10 K higher than CH<sub>3</sub>CH=CH<sub>2</sub> from (CH<sub>3</sub>)<sub>2</sub>CHOH. Other oxidation products such as acetone (monitored at 43 and 58 amu after subtraction of 2-propanol fragments) and isopropyl ether (87 amu) are not observed.

The effect of the TiO<sub>2</sub>(110) substrate on the catalytic activity of (WO<sub>3</sub>)<sub>3</sub> is determined by varying the cluster preparation conditions. In condition A, the (WO<sub>3</sub>)<sub>3</sub> clusters are allowed to interact with multilayers of 2-propanol and land on TiO<sub>2</sub>(110) only after the excess 2-propanol desorbs at ~200 K. This experiment aims to model the reactivity of unsupported, isolated (WO<sub>3</sub>)<sub>3</sub> clusters. In condition B, the clusters are deposited onto TiO<sub>2</sub>(110) at 100 K and subsequently exposed to excess 2-propanol. In condition C, the clusters of condition B are annealed to 600 K before the 2-propanol exposure.

The propene TPD spectra obtained in the 2-propanol dehydration experiments described above are shown in Figure 2. Surprisingly, the maximum propene desorption rate occurs at the same temperature for all three cases. The unchanged desorption temperature indicates that the activation energy for the dehydration is practically unaffected by the cluster proximity and/or binding to TiO<sub>2</sub>(110). A small broadening of the desorption peak occurs from spectrum A to B with the appearance of an additional high temperature shoulder (~480 K) on spectrum C. In contrast with relatively subtle changes in the desorption line shape, the total propene yield is found to decrease 3 times from spectrum A to B, and an additional 4 times from spectrum B to C. For comparison, a propene TPD spectrum from 2-propanol dehydration on clean TiO<sub>2</sub>(110) is also shown (panel D, Figure 2). The dehydration channel (~570 K) on bridge-bonded oxygen (BBO) vacancies (BBO<sub>v</sub>'s) of clean TiO<sub>2</sub>(110)<sup>10,11,17</sup> is completely suppressed for spectra A–C indicating that the contribution of the substrate to the overall catalytic activity is rather small.

The relationship between the cluster coverage and the dehydration yield is further investigated in Figure 3 showing the total yield of propene produced by the dehydration of 2-propanol on (WO<sub>3</sub>)<sub>3</sub> clusters prepared via procedures A, B, and C. For case A, the number of propene molecules produced per deposited (WO<sub>3</sub>)<sub>3</sub> is found to be six for all studied (WO<sub>3</sub>)<sub>3</sub> coverages, suggesting that each W=O group is available to react with one 2-propanol molecule. For case B, the ratio is found to vary from four at very low coverages (<0.7 (WO<sub>3</sub>)<sub>3</sub> nm<sup>-2</sup>) to two as the coverage increases to a full monolayer (~1.8 (WO<sub>3</sub>)<sub>3</sub> nm<sup>-2</sup>). For multilayer (WO<sub>3</sub>)<sub>3</sub> coverages, the ratio further monotonically decreases since

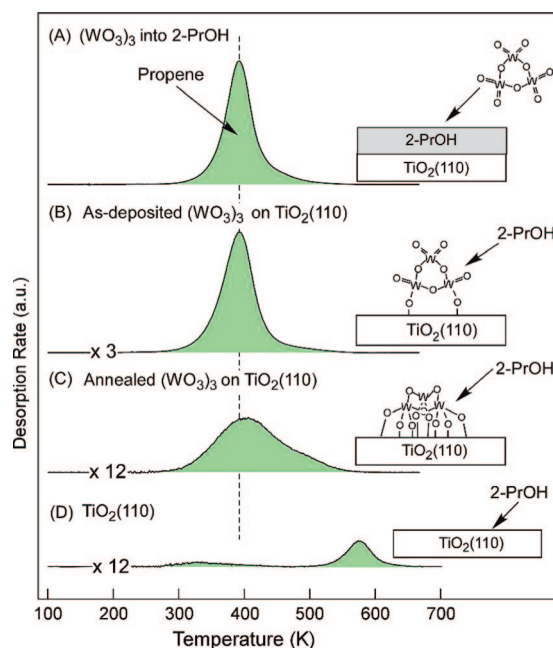


**Figure 2.** Propene TPD spectra (tracked at 41 amu) resulting from 2-propanol dehydration on (WO<sub>3</sub>)<sub>3</sub> clusters. (A) (WO<sub>3</sub>)<sub>3</sub> clusters are deposited into multilayers of 2-propanol (18 nm<sup>-2</sup>) on TiO<sub>2</sub>(110); (B) (WO<sub>3</sub>)<sub>3</sub> clusters are deposited onto TiO<sub>2</sub>(110) at 100 K and subsequently exposed to 2-propanol (18 nm<sup>-2</sup>); (C) clusters from condition B are annealed to 600 K and exposed to 18 nm<sup>-2</sup> of 2-propanol; (D) dehydration of 15 nm<sup>-2</sup> of 2-propanol on clean TiO<sub>2</sub>(110) is also shown for comparison.

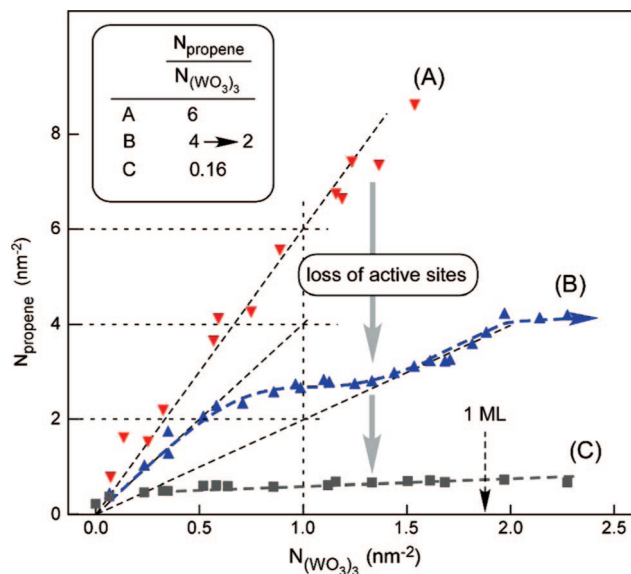


**Figure 3.** Propene yield,  $N_{\text{propene}}$ , vs (WO<sub>3</sub>)<sub>3</sub> coverage,  $N_{(\text{WO}_3)_3}$ , for the clusters A, B, and C prepared as described in the caption of Figure 2. Straight dotted lines with the slope of 2, 4, and 6 are drawn to guide the eye.

only a fraction of deposited (WO<sub>3</sub>)<sub>3</sub> clusters are exposed to 2-propanol. The data suggest that isolated supported clusters (low coverage limit) have four available W=O groups for the reaction while the remaining two are blocked by contact with the TiO<sub>2</sub>(110) surface. It is likely that as the cluster coverage increases, cluster–cluster interactions involve additional W=O groups leading to the decreased availability of catalytically active W=O groups.

Strikingly, the 600 K preannealed (WO<sub>3</sub>)<sub>3</sub> clusters, (C), show a dramatically lower catalytic activity with a yield of ~0.16 propene per (WO<sub>3</sub>)<sub>3</sub>. On the basis of our prior STM study of 450–600 K annealed (WO<sub>3</sub>)<sub>3</sub> clusters on TiO<sub>2</sub>(110) we expected the yield to



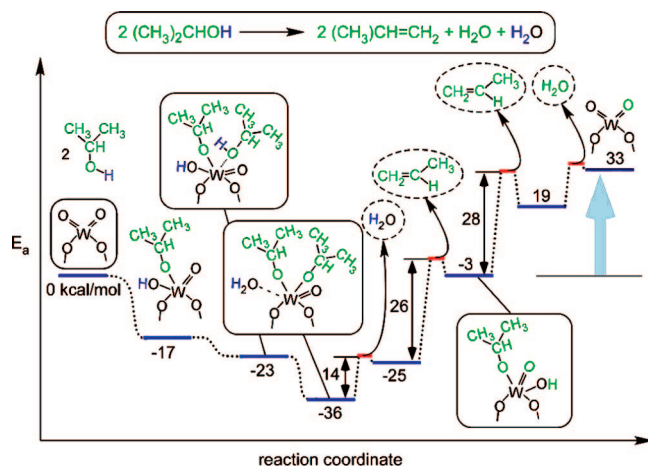


**Figure 4.** Calculated potential energy diagram for catalytic dehydration of two 2-propanol over  $(\text{WO}_3)_3$  clusters.

be  $\sim 4$  propene per  $(\text{WO}_3)_3$  since our proposed model involved  $(\text{WO}_3)_3$  bound with two tungstyl groups.<sup>5,6</sup> The exact origin of this low activity is not clear. We speculate that it is a result of the partial loss of active  $\text{W}=\text{O}$  perhaps due to thermal decomposition of the clusters during the dehydration reaction. This conclusion is consistent with the results of the DFT simulations discussed below. Our future STM studies of the cluster morphology before and after the dehydration reaction are aimed to address this issue. Subsequent TPD experiments after additional 2-propanol adsorptions show that the reactivity of 600 K annealed clusters remains unchanged.

To ascertain a viable mechanism for the dehydration process we have performed DFT calculations on an isolated  $(\text{WO}_3)_3$ . Only the relevant steps that lead directly from the initial reagent, 2-propanol, to the final products, water and propene via the lowest energy route, are reported. The resulting diagram with the energetics of all key intermediates and activation energies for each step is shown in Figure 4. In agreement with the thermodynamic data, the dehydration reaction is endothermic with an energy gain of 33 kcal/mol. Further, the energy barrier for noncatalyzed dehydration of 2-propanol is very high ( $\sim 70$  kcal/mol). For the cluster-catalyzed reaction the highest barrier of any step is 28 kcal/mol and the overall energy required is given by the endothermicity of the process.

The initial adsorption and dissociation of two alcohol molecules is barrierless and significantly exothermic ( $-23$  kcal/mol). Deprotonation of both alcohols follows with relatively low barriers (5–10 kcal/mol) to form  $\text{H}_2\text{O}$ . This process is also exothermic and leads to the lowest energy configuration on the diagram which is 36 kcal/mol lower than the initial reactants and exhibits an increased coordination of the  $\text{W}(\text{VI})$  from 4 to 6 with two BBO's, one  $\text{H}_2\text{O}$ , one  $\text{W}=\text{O}$ , and two 2-propoxy groups. All subsequent steps are endothermic, the first being the release of a water molecule with a kinetic barrier of 14 kcal/mol. The following step is rupture of the  $\text{C}-\text{O}$  bond of the propoxy with simultaneous transfer of the  $\beta$ -H from a methyl group. This step occurs twice concurrently (once for each propoxy) and exhibits the highest activation energy. The final step is the release of an additional water molecule and regeneration of the original  $(\text{WO}_3)_3$  cluster. The barriers for the computed steps are in good agreement with the experimental observations. The first water formed from the deprotonated propanols is released as a first product between 200 and 350 K followed by propene formation between 300 and 500 K. A simple simulation of the first order desorption process with a typical value of prefactor of  $10^{13} \text{ s}^{-1}$  and activation barriers of 14 and 26–28 kcal/mol determined theoretically for the low temperature water

desorption and alkene formation, yields desorption spectra with maxima at 240 and 405–432 K, in excellent agreement with the experimentally observed values of 250 and 400 K, respectively.

We have also addressed changes in the dehydration mechanism as a result of cluster-surface interactions by simulating the  $(\text{WO}_3)_3$  cluster molecularly adsorbed on  $\text{TiO}_2(110)$ . The lowest energy configuration, bound by 22 kcal/mol, forms 2  $\text{Ti}-\text{O}$  bonds with the  $\text{W}=\text{O}$  groups of the cluster in accord with prior interpretation of our STM data.<sup>5,6</sup> The mechanism of the dehydration reaction on such supported  $(\text{WO}_3)_3$  clusters is very similar to that for the isolated  $(\text{WO}_3)_3$  with only small variations in the energetics.

Molecular dynamics simulations at 1000 K show that the molecularly adsorbed  $(\text{WO}_3)_3$  is not the lowest energy configuration and that it further decomposes into a chainlike structure on the surface, opening the cluster ring and losing a  $\text{W}=\text{O}$  group, during the course of a short (1 ps) simulation. The cluster dissociation has an appreciable energy barrier of about 30 kcal/mol and results in a structure that is 11 kcal/mol lower in energy and indicates that high temperature annealing of the system may well result in the decomposition of clusters.

In conclusion our study of the  $(\text{WO}_3)_3/\text{TiO}_2(110)$  model system provides deep insight into the mechanism of alcohol dehydration which is likely applicable to more complex supported high surface area tungsten trioxide catalysts with  $\text{W}=\text{O}$  bonds being the primary reaction sites. Our studies suggest that  $(\text{WO}_3)_3$  is an extremely efficient catalyst for dehydration of alcohols, effectively lowering the energy barrier as much as possible for an endothermic reaction.

**Acknowledgment.** This work was supported by the U.S. Department of Energy Office of Basic Energy Sciences, Chemical Sciences and Materials Sciences Divisions, Robert A. Welch Foundation (F-0032) and National Science Foundation (Grant CHE-0412609) and performed at W. R. Wiley Environmental Molecular Science Laboratory, a national scientific user facility sponsored by the Department of Energy's Office of Biological and Environmental Research located at Pacific Northwest National Laboratory (PNNL). PNNL is operated for the U.S. DOE by Battelle Memorial Institute under Contract No. DE-AC06-76RLO 1830.

## References

- Baertsch, C. D.; Komala, K. T.; Chua, Y. H.; Iglesia, E. *J. Catal.* **2002**, *205*, 44.
- Chen, K. D.; Bell, A. T.; Iglesia, E. *J. Catal.* **2002**, *209*, 35.
- Lebarbier, V.; Clet, G.; Houalla, M. *J. Phys. Chem. B* **2006**, *110*, 13905.
- Kustov, A. L.; Egeblad, K.; Kustova, M.; Hansen, T. W.; Christensen, C. H. *Top. Catal.* **2007**, *45*, 159.
- Bondarchuk, O.; Huang, X.; Kim, J.; Kay, B. D.; Wang, L. S.; White, J. M.; Dohnálek, Z. *Angew. Chem., Int. Ed.* **2006**, *45*, 4786.
- Kim, J.; Bondarchuk, O.; Kay, B. D.; White, J. M.; Dohnálek, Z. *Catal. Today* **2007**, *120*, 186.
- Maleknia, S.; Brodbelt, J.; Pope, K. *J. Am. Soc. Mass Spectrom.* **1991**, *2*, 212.
- Huang, X.; Zhai, H. J.; Kiran, B.; Wang, L. S. *Angew. Chem., Int. Ed.* **2005**, *44*, 7251.
- Sun, Q.; Rao, B. K.; Jena, P.; Stolcic, D.; Kim, Y. D.; Gantefor, G.; Castleman, A. W. *J. Chem. Phys.* **2004**, *121*, 9417.
- Bondarchuk, O.; Kim, Y. K.; White, J. M.; Kim, J.; Kay, B. D.; Dohnálek, Z. *J. Phys. Chem. C* **2007**, *111*, 11059.
- Kim, Y. K.; Kay, B. D.; White, J. M.; Dohnálek, Z. *J. Phys. Chem. C* **2007**, *111*, 18236.
- Dohnálek, Z.; Kim, J.; Bondarchuk, O.; White, J. M.; Kay, B. D. *J. Phys. Chem. B* **2006**, *110*, 6229.
- Perdew, J. P.; Burke, K.; Ernzerhof, M. *Phys. Rev. Lett.* **1996**, *77*, 3865.
- Lippert, G.; Hutter, J.; Parrinello, M. *Mol. Phys.* **1997**, *92*, 477.
- VandeVondele, J.; Krack, M.; Mohamed, F.; Parrinello, M.; Chassaing, T.; Hutter, J. *Comput. Phys. Commun.* **2005**, *167*, 103.
- Mills, G.; Jonsson, H.; Schenter, G. K. *Surf. Sci.* **1995**, *324*, 305.
- Kim, Y. K.; Kay, B. D.; White, J. M.; Dohnálek, Z. *Catal. Lett.* **2007**, *119*, 1.

JA800730G